

Electronic supplementary information (ESI)

Reduction of intracellular oxidative stress with copper incorporated layered double hydroxide nanozymes

Adél Szerlauth,^a Tamara Madácsy,^b Gergely Ferenc Samu,^c Péter Bíró,^d Miklós Erdélyi,^d Gábor Varga,^e Zhi Ping Xu,^f József Maléth^b and István Szilágyi^{*a}

^aMTA-SZTE Momentum Biocolloids Research Group, Interdisciplinary Excellence Center, University of Szeged, H-6720 Szeged, Hungary

^bMTA-SZTE Momentum Epithelial Cell Signaling and Secretion Research Group, Interdisciplinary Excellence Center, University of Szeged, H-6720 Szeged, Hungary

^cDepartment of Molecular and Analytical Chemistry, University of Szeged, H-6720 Szeged, Hungary

^dDepartment of Optics and Quantum Electronics, University of Szeged, H-6720 Szeged, Hungary

^eDepartment of Applied and Environmental Chemistry, University of Szeged, H-6720 Szeged, Hungary

^fAustralian Institute for Bioengineering and Nanotechnology, The University of Queensland, QLD-4072 Brisbane, Australia

*E-mail: szistvan@chem.u-szeged.hu

EXPERIMENTAL

Materials

Magnesium chloride hexahydrate ($\text{MgCl}_2 \times 6 \text{H}_2\text{O}$), aluminium chloride hexahydrate ($\text{AlCl}_3 \times 6\text{H}_2\text{O}$), copper chloride dihydrate ($\text{CuCl}_2 \times 2\text{H}_2\text{O}$), sodium hydroxide pellet (NaOH), hydrogen peroxide (H_2O_2 , 30 wt%), sodium chloride (NaCl), ammonium molybdate (para) tetrahydrate, anhydrous disodium hydrogen phosphate (Na_2HPO_4), sodium dihydrogen phosphate (NaH_2PO_4), xanthine, nitro blue tetrazolium chloride monohydrate (NBT), and the 96 well black microplate were purchased from VWR International. Xanthine oxidase, HEPES buffer, menadione, 2',7'-dichlorodihydrofluorescein diacetate (H_2DCFDA) and Triton X100 were obtained from Sigma Aldrich. Dulbecco's modified eagle medium (DMEM), 10 % fetal bovine serum (FBS), 1% kanamycin, Gluta Max supplement and phosphate buffer (PBS) were purchased from Gibco. Human cervical adenocarcinoma (HeLa) cells were obtained from ATCC, apoptosis/necrosis detection assay kit and reactive oxygen species (ROS)/superoxide detection assay kit from Abcam, cell view slide from Greiner Bio-One, while CellTiter-Glo® 3D cell viability assay kit from Promega. The reagents were in analytical grade, while ultrapure water was obtained by an ADRONA B30 water purification system.

Synthesis of copper containing layered double hydroxide (LDH) nanoparticles

The $\text{Cu}_x\text{Mg}_{3-x}\text{Al}$ LDH particles were synthesized by flash coprecipitation followed by hydrothermal treatment.¹ The ratio of divalent and trivalent metal cations was set to 3:1, while the copper(II)-to-magnesium(II) ratio was systematically varied ($x = 0.2, 0.4, 0.6$). The metal salts were dissolved in 5 mL ultrapure water to obtain solutions of 0.8 M total metal concentration and then added to 20 mL of 0.4 M NaOH solution. After 40 minutes of vigorous stirring, the sample was centrifuged and washed twice. The slurry was redispersed in 20 mL ultrapure water, then transferred to an autoclave and treated at 100 °C overnight. The sample was centrifuged and the supernatant was used in further experiments.

Sample characterization techniques

The X-ray diffractograms were collected with a Bruker D8 Advanced diffractometer, operating at $\lambda = 0.1542$ nm and 40 kV voltage. The diffractograms were recorded in the 5 – 80 2θ range, with 0.02° steps. Basal spacing (d) was calculated based on the Bragg's law:²

$$n \cdot \lambda = 2d \cdot \sin\theta \quad (\text{S1})$$

where n is the diffraction order, and θ is the angle of incidence. The crystal parameters were calculated as follows:

$$\frac{1}{d_{hkl}^2} = \left[\frac{4}{3} \cdot (h^2 + k^2 + h \cdot k) + l^2 \cdot \left(\frac{a}{c} \right)^2 \right] \cdot \frac{1}{a^2} \quad (\text{S2})$$

where a and c are the crystal parameters, while h , k and l defines the orientation of the distinguished plane.

The hydrodynamic diameter, polydispersity index and zeta potential of the samples were determined in aqueous dispersions at a particle concentration of 10 mg/L using a Nano Zeta-Sizer (Malvern Instruments) instrument, which can be used in both electrophoretic and dynamic light scattering modes.³ During the measurements, 1 mM NaCl was used as background electrolyte to control the thickness of the electrical double layer.

Raman spectra were collected with a Bruker Senterra II Raman microscope having a light source of 532 nm wavelength and 12.5 mW laser power. Final data were obtained by averaging 16 spectra with an exposition time of 10 seconds.

A SPECS instrument equipped with a PHOIBOS 150 MCD 9 hemispherical analyser was used to perform X-ray photoelectron spectroscopy (XPS) measurements for surface analysis. The electron energy analyser was operated in fixed analyser transmission (FAT) mode with 40 eV pass energy for acquiring survey scans and 20 eV for high resolution scans. Al $K\alpha$ radiation ($h\nu = 1486.6$ eV) was used as an excitation source and operated at 150 W power. An electron flood-gun was used to compensate for sample charging (adventitious carbon 1s peak was monitored and set at 284.8 eV). Each sample contained some amount of adventitious carbon

adsorbed on the sample surface, which was used as an internal standard for charge referencing. For spectrum evaluation, CasaXPS commercial software package was used.⁴

Time-correlated single photon counting (TCSPC) based fluorescence lifetime microscopy (FLIM) measurements were performed with a PicoQuant upgrade kit installed into a (LSM) Nikon C2+ laser scanning confocal unit. The sample was excited with a picosecond laser diode operating at 560 nm with a repetition rate of 20 MHz. The sample was scanned with a high numerical aperture objective (Nikon CFI Plan Apo Lambda 60x Oil, NA:1.4), and the emitted fluorescence light was spectrally filtered with a bandpass filter (ET600/50m, Chroma). The emitted single photons were collected with a PMA Hybrid 40 detector unit having <120 ps response time and >40% detection efficiency. During the measurements, the dimensions of the area to be scanned typically equaled to $30 \times 30 \mu\text{m}^2$ (256×256 pixels), and $>10^5$ photons were collected for precise lifetime calculations. The liquid sample was mounted on a cavity microscope slide and covered with a standard ($170 \mu\text{m}$ thick) microscope coverslip. To avoid surface-induced artifacts, all data were collected $>5 \mu\text{m}$ above the coverslip, where the sample was assumed to be homogeneous. Based on the Einstein equation, one can assume that during the fluorescence lifetime (<10 ns), the nanoparticle remains inside the excited volume determined by the 3D point spread function of the imaging system. All post processing evaluations were performed using the SymPhoTime 64 software (PicoQuant).

Enzyme activity

A simple spectrophotometric assay based on the reaction between ammonium molybdate and H_2O_2 was used to determine the catalase (CAT) activity of the nanozymes.⁵ The total volume of the reaction mixture was adjusted to 2.5 mL. The H_2O_2 concentration was fixed at 3 mM, while the nanozyme concentration was systematically varied in the range of 0 – 300 mg/L, while the activity of MA sample was monitored at 300 mg/L particle concentration. Three minutes after mixing the H_2O_2 with the nanozyme dispersion, the reaction was stopped by

adding the required amount of ammonium molybdate solution (the concentration in the reaction mixture was set to 25.4 mM). The ammonium molybdate reacts with H₂O₂ to produce a yellow-coloured complex, which has an absorbance maximum at 350 nm wavelength. By monitoring the absorbance at this wavelength, the remaining H₂O₂ (H₂O₂ (%)), i.e., the amount of substrate, which was not decomposed by the nanozyme, was calculated as:

$$\text{H}_2\text{O}_2 (\%) = \frac{A - A_p}{A_0} \quad (\text{S3})$$

where A is the absorbance measured after the reaction was terminated, A_p , is the absorbance derived from the scattering of particle dispersion, while A_0 is the absorbance of the H₂O₂ and ammonium molybdate complex. The efficient concentration (EC₅₀) value was determined from the H₂O₂ (%) versus catalyst concentration plots. Note that EC₅₀ is the nanozyme concentration needed for the decomposition of 50 % of the H₂O₂ in the cuvette.

To evaluate the superoxide dismutase activity, the Fridovich assay was applied.⁶ The final reaction mixture contained 0.2 mM xanthine, 0.1 mM NBT and 0.3 g/L xanthine oxidase in phosphate buffer (the final concentration of the phosphate buffer in the reaction mixture was 1 mM and the pH was adjusted to 7), which was completed to 1.5 mL with the nanozyme dispersion. The nanozyme concentration was systematically varied in the range of 0 – 6 mg/L, while concentration of MA was set to 6 mg/L. After mixing the components, absorbance was monitored at 565 nm for 6 minutes. Inhibition (I) was calculated from the change in absorbance with (ΔA) and without (ΔA_0) nanozyme dispersion:

$$I = \frac{\Delta A - \Delta A_0}{\Delta A_0} \quad (\text{S4})$$

The I values were plotted against nanozyme concentration, and IC₅₀ data were determined based on a mathematical function fitted to the points. The IC₅₀ is the enzyme concentration necessary to decompose half of the superoxide radical ions forming during the test. The average error of the above enzymatic assays is 10 %.

Cell lines

HeLa cells (Cat. No.: ATCC-CCL-2) respectively were grown in DMEM/F12 containing 10% fetal bovine serum (FBS), 1 % Kanamycin, 1 % Penicillin-Streptomycin and 1% GlutaMax supplement.⁷ Cells were seeded to 70-80% of confluency before experiments.

Detection of Apoptosis/Necrosis

Cell viability with Apoptosis/Necrosis detection kit (blue, green, red) (Cat No.: ab176749) is used to simultaneously monitor apoptotic, necrotic, and healthy cells. The phosphoserine (PS) sensor used in this kit has green fluorescence (Ex/Em = 490/525 nm) upon binding to membrane PS. Loss of plasma membrane integrity, as demonstrated by the ability of a membrane-impermeable 7-AAD (Ex/Em = 546/647 nm) to label the nucleus is the marker of apoptosis, and CytoCalcein Violet 450 (Ex/Em = 405/450 nm), labels the cytoplasm of living cells. Cells were grown on a CELLview Slide (Greiner Bio-One; Cat. No.: 543079) in a humidified incubator at 37°C. When cells reached optimal confluency they were washed 2x with pre-warmed Hepes buffer. Tested compounds were applied to the wells in final concentrations in 37°C Hepes. Cells are co-incubated with the compounds for 1h in a humidified incubator at the same temperature. After incubation, the cells are washed once with warm Hepes solution. Apoptosis/Necrosis detection kit components were mixed following the manufacturers protocol then added to the wells. Cells were incubated with the concoction for 30 minutes in a humidified incubator at 37°C. After incubation, cells were washed from the reaction mixture 3-time in warm Hepes and then, immediately visualized with a Zeiss LSM 880 confocal microscope.

CellTiter-Glo® 3D cell viability assay

The CellTiter-Glo® 3D Cell Viability Assay (Cat. No.: G9681) is a homogeneous method to determine the number of viable cells in cell culture based on quantification of the adenosine triphosphate (ATP) present, which is a marker for the presence of metabolically active cells. The amount of ATP is directly proportional to the number of viable cells present in the culture. The CellTiter-Glo® 3D Cell Viability Assay relies on the properties of a proprietary

thermostable luciferase (Ultra-Glo™ Recombinant Luciferase), which generates a stable “glow-type” luminescent signal and improves performance across a wide range of assay conditions. CellTiter-Glo® 3D Cell Viability Assay was removed from -20°C and placed to 4°C overnight. Assay buffer was equilibrated at room temperature 30 minutes prior experiments. HeLa cells were plated onto a white, flat-bottomed microplate (Cat.No: 655083) at 1×10^4 cell/well density. When cells reached 80%-90% confluency, briefly; cells were washed with warm sterile DPBS once to remove culturing media. Supernatant was removed then cells were treated with the final concentration of compounds in warm Hepes for 1 hour at 37°C in a humidified atmosphere. Supernatant was removed, then cells were washed in fresh pre-warmed Hepes. Room temperature CellTiter-Glo® 3D reagent was added to the wells in 100 μ L volume/well amount. Microplates were then placed into a BMG Fluostar Optima Microplate Reader at room temperature. After shaking the assay for 5 minutes, it was left for a 25-minute activation time, according to the Promega protocol. Measurement was started after the recommended activation time. Data were normalised to protein mass concentration of each sample measured by Bradford protein assay as follows. First, 10-time dilution was made from each of the samples measured in the CellTiter-Glo® 3D cell viability assay. Then, 196 μ L of Bradford reagent and 4 μ L of 10-time diluted sample were added to each well of a flat bottom and transparent microplate. The microplate was inserted into a BMG Fluostar Optima microplate reader at room temperature, and the measurement was started after 5 minutes and gentle agitation. Endpoint was measured at 595 nm wavelength.

Evaluation of intracellular ROS levels in HeLa cells by fluorescent microscopy

Changes in intracellular ROS level were measured by loading the cells with 5 μ M 2',7'-dichlorodihydrofluorescein diacetate (H₂DCFDA) for 30 minutes. HeLa cells were grown to a glass coverslip (24 mm diameter) as the base of a perfusion chamber and were mounted on the stage of an Olympus IX71 inverted microscope. Cells were bathed with different external

solutions at 37°C at the perfusion rate of 2-3 mL/minute. Region of interests (ROIs) were determined by the Excellence software (Olympus) and changes of intracellular ROS were determined by exciting the cells with an MT20 light source equipped with a ~492–495 nm excitation filters. Excitation and emission wavelengths were separated by a 400 nm beam splitter and the emitted light were captured with a Hamamatsu ORCA- ER CCD camera with one measurement per second rate. During further analysis, the fluorescence signals were normalized to the initial fluorescence intensity (F1/F0) and expressed as relative fluorescence.

Determining intracellular oxidative stress and superoxide levels

The ROS/superoxide detection assay kit (Cat No. ab139476) is designed to monitor real time ROS production in live cells using fluorescence microplate reader. The protocol is based on two fluorescent dyes. Namely, oxidative stress detection reagent (Green, Ex/Em 490/525 nm) for the determination of total ROS, and superoxide detection reagent (Orange, Ex/Em 550/620 nm) to detect the superoxide radicals. The HeLa cells were grown on a glass bottom 96 well black microplate (Cat No. 7341609) in 1×10^4 cell/well density. All treatments were carried out at 37°C at a humidified atmosphere. Cells were treated with each compound at sufficient concentrations for 1 hour, then the cells were washed once with pre-warmed Hepes. In addition, cells were treated for 15 minutes with 50 μ M menadione followed by a 30 minutes incubation with the oxidative stress/superoxide detection mixture according to the manufacturer's protocol. Changes in intracellular fluorescence levels were detected by a BMG Optima Fluostar Microplate Reader at Green, (Ex/Em 490/525 nm) and Orange, (Ex/Em 550/620 nm) channels.

Statistical analysis of cellular measurements

The GraphPad Prism software was used for statistical analysis of the measurements and to determine the strength of significance. All data were expressed as \pm standard error of the mean. Both parametric and nonparametric tests based on the normality of the data distribution were used. The P values less than 0.05 were considered to be statistically significant.

Table S1. Lattice parameters, hydrodynamic diameters, polydispersity indices and zeta potential data of the synthesized nanoparticles.

Sample	$2\theta(003) / ^{\circ}$ ^a	$d(003) / \text{\AA}$ ^b	$c / \text{\AA}$ ^c	D_h / nm ^d	PDI ^e	ζ / mV ^f
MA	11.6	8.39	25.17	77.1 ± 5.2	0.214	32.1 ± 2.2
CMA1	11.4	8.54	25.61	84.8 ± 0.1	0.241	31.0 ± 0.8
CMA2	11.4	8.54	25.61	82.9 ± 0.2	0.229	28.4 ± 1.1
CMA3	11.4	8.54	25.61	89.4 ± 0.7	0.237	32.3 ± 0.4

^a 2θ value corresponds to the (003) Miller index. ^bThe basal spacing was calculated with Eq S1.

^cCrystal parameters were obtained from Eq S2. ^d D_h is the hydrodynamic diameter, ^ePDI is the polydispersity index, while ^f ζ is the zeta potential of the particles, measured at 10 mg/L particle concentration and 1 mM ionic strength.

Table S2. Binding energies of Cu 2p_{3/2} region in the XPS spectra.

Sample	<i>Cu(I)</i> 2p _{3/2} / eV	<i>Cu(II)</i> 2p _{3/2} / eV
		-
MA	-	-
		-
		-
		934.40
CMA1	931.75	939.03
		941.93
		943.85
		934.39
CMA2	931.75	939.02
		941.92
		943.85
		934.31
CMA3	931.71	938.94
		941.84
		943.76
		934.67
Reference		939.30
s ⁸⁻¹⁰	932.18	942.20
		944.12

Table S3. Binding energies of Mg 2p and Al 2p regions of XPS spectrum.

Sample	<i>Mg(II) 2p</i> / eV	<i>Al(III) 2p</i> / eV
MA	49.72	74.30
CMA1	49.67	74.23
CMA2	49.67	74.13
CMA3	49.62	74.06
References ⁸⁻¹⁰	49.4	74.0

Table S4. Surface elemental composition of MA and CMA1-3 determined by XPS.

Sample	Mg / at%	Al / at%	Cu / at%	Surface stoichiometric ratio
MA	79.1	20.9	-	Mg _{3.16} Al _{0.84}
CMA1	73.9	24.3	1.8	Mg _{2.96} Al _{0.97} Cu _{0.07}
CMA2	73.9	23.7	2.3	Mg _{2.96} Al _{0.95} Cu _{0.09}
CMA3	71.8	24.7	3.5	Mg _{2.87} Al _{0.99} Cu _{0.14}

The values are given in at%, which represents the atomic percentage of the relevant species to indicate the different metal content of the samples.

Table S5. EC₅₀ and IC₅₀ values calculated based on the CAT and Fridovich (SOD) assay.

Sample	EC ₅₀ / mg/L ^a	IC ₅₀ / mg/L ^b
MA	N/A ^c	N/A ^c
CMA1	165	0.68
CMA2	136	0.43
CMA3	149	0.52
SOD ^d	N/A	0.053
CAT ^d	0.66	N/A

^aEC₅₀ values were calculated by the CAT assay, while ^bIC₅₀ values are determined in the Fridovich assay. The average error of the enzymatic tests is 10 %. ^cN/A means, that the particle was inactive. ^dThe activity of the native enzymes reported earlier⁷ were reproduced within experimental error.

Table S6. CAT and SOD activity for various nanozymes.

Sample	Activity		Ref.
	SOD-like	CAT-like	
Au@Cu ₂ O ^a	O ₂ ^{•-} elimination (5 mg/L): < 20 %	bubble formation, no quantitative data	11
MnO ₂ -BSA ^b	Inhibition rate (5mg/L): < 20 %	Inhibition rate (40 mg/L): ~ 50 %	12
MoS ₂ @TiO ₂ ^c	O ₂ ^{•-} elimination (50 mg/L) ~ 50%	Decrease in fluorescence (3.75 mg/L): ~ 50%	13
RuO ₂ NPs ^d	O ₂ ^{•-} elimination (5 mg/L): ~50%	H ₂ O ₂ elimination after 3 minutes (20 mg/L): ~ 30%	14
V ₂ O ₅ @pDA@MnO ₂ ^e	O ₂ ^{•-} inhibition (5mg/l): ~ 60%	no quantitative data	15
m-CoAl LDH ^f	Inhibition rate (5mg/L): ~ 30%	–	16
Ru ₁ /LDH ^g	Inhibition (40 mM): ~ 80%	bubble formation, no quantitative data	17

^aCu₂O coated Au nanorod. ^bBovine serum albumin coated MnO₂ nanoparticles. ^cMoS₂-coated TiO₂ nanobelt. ^dRuO₂ nanoparticles. ^eV₂O₅ nanowire linked to MnO₂ nanoparticles with dopamine linker. ^fVacancies-rich CoAl LDH monolayers. ^gMgAl LDH supported Ru single-atom nanozyme.

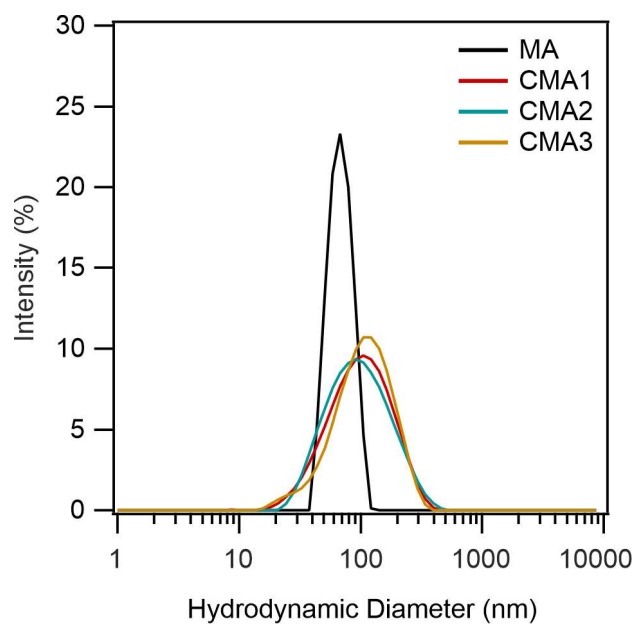


Fig. S1 Intensity-weighted hydrodynamic size distribution diagrams of MA, CMA1, CMA2 and CMA3 determined by dynamic light scattering.

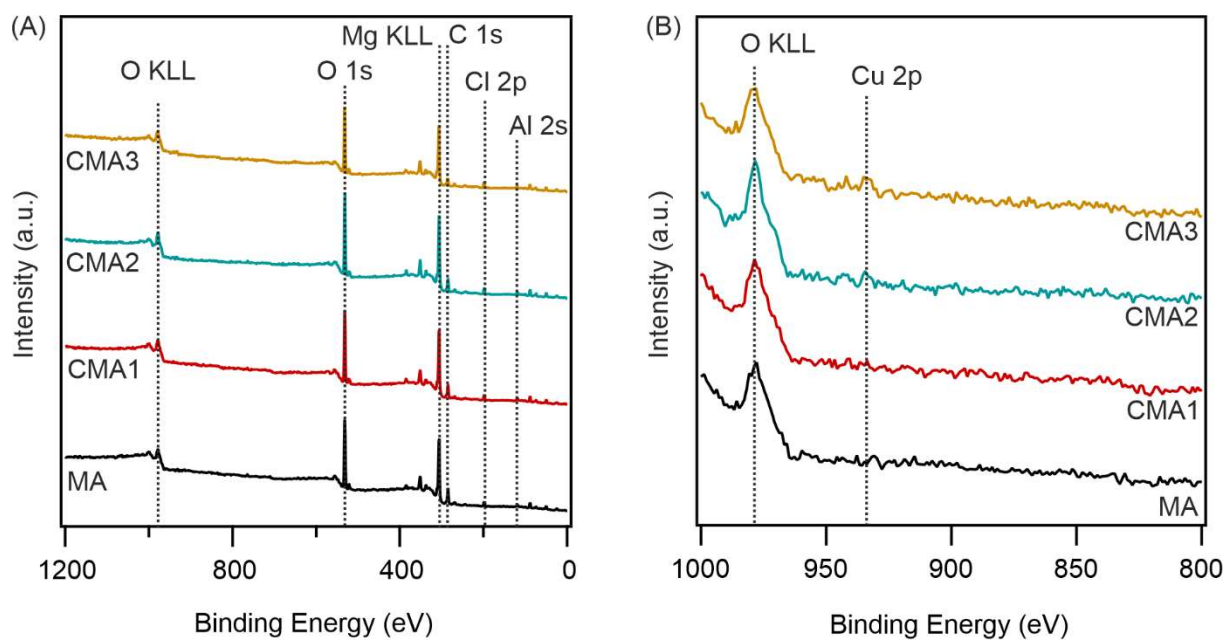


Fig. S2 Full survey scan (A) and in the 1000 – 800 eV range (B) recorded for the MA and CMA samples.

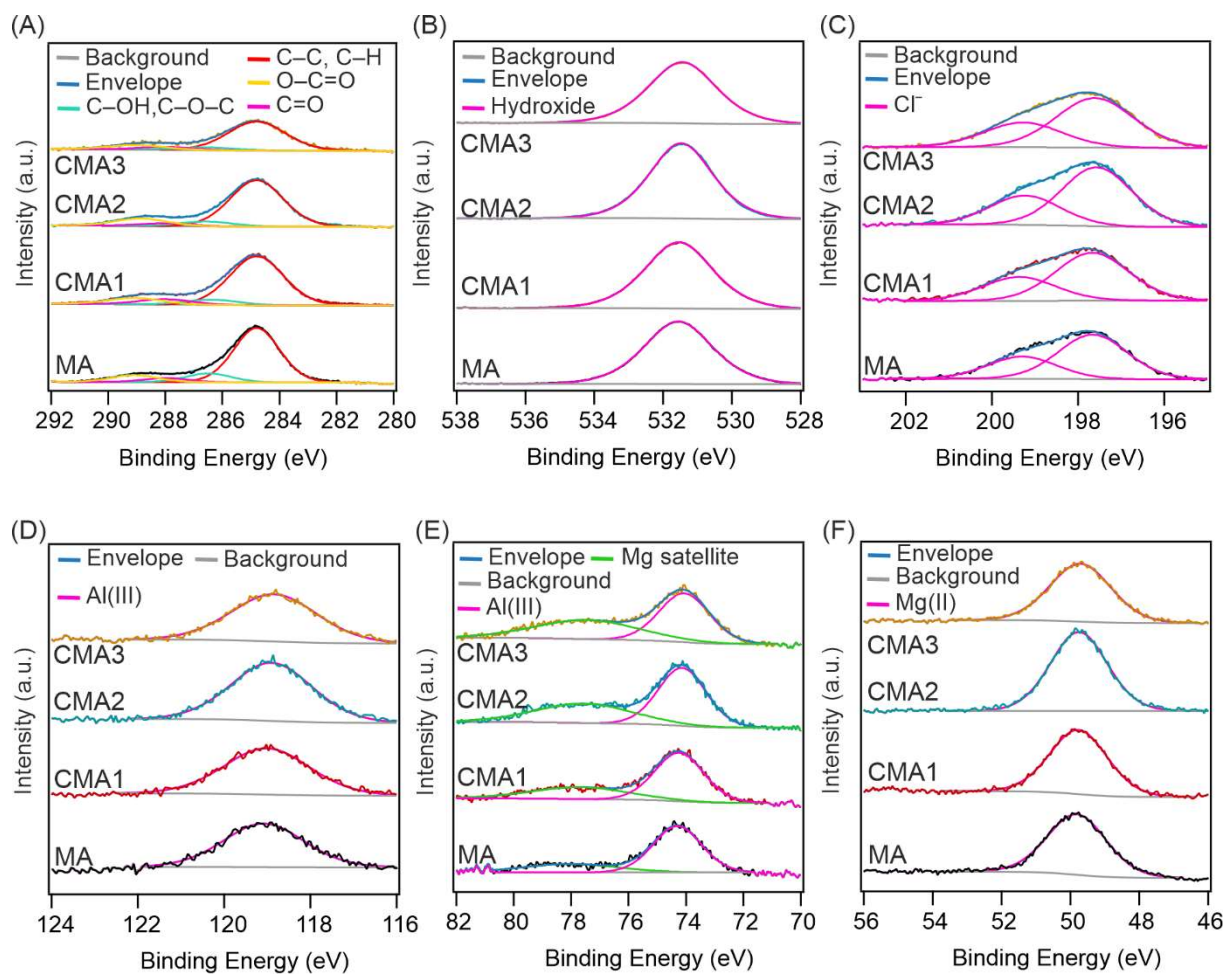


Fig. S3 XPS spectra of the region related to C 1s (A), O 1s (B), Cl 2p (C), Al 2s (D), Al 2p (E) and Mg 2p (F).

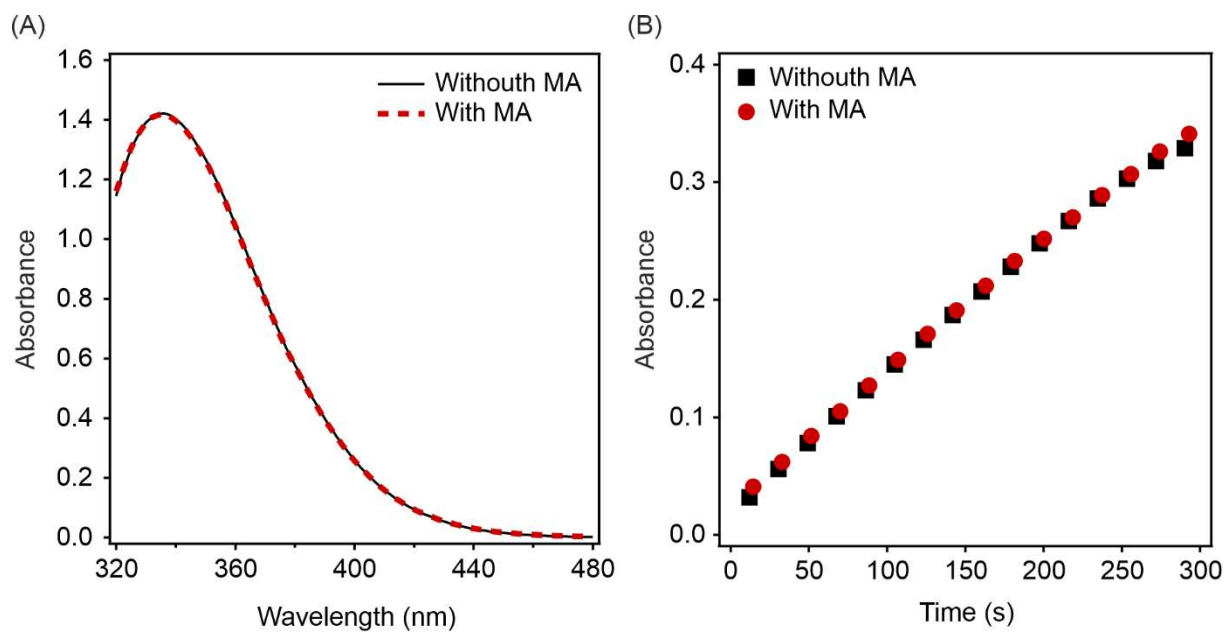


Fig. S4 UV-Vis spectra determined during CAT assay without and with 300 mg/L MA (A). Change in absorbance at 565 nm wavelength in SOD assay without and with 6 mg/L MA (B). The overlaps in the data clearly indicate the inactivity of MA in these assays.

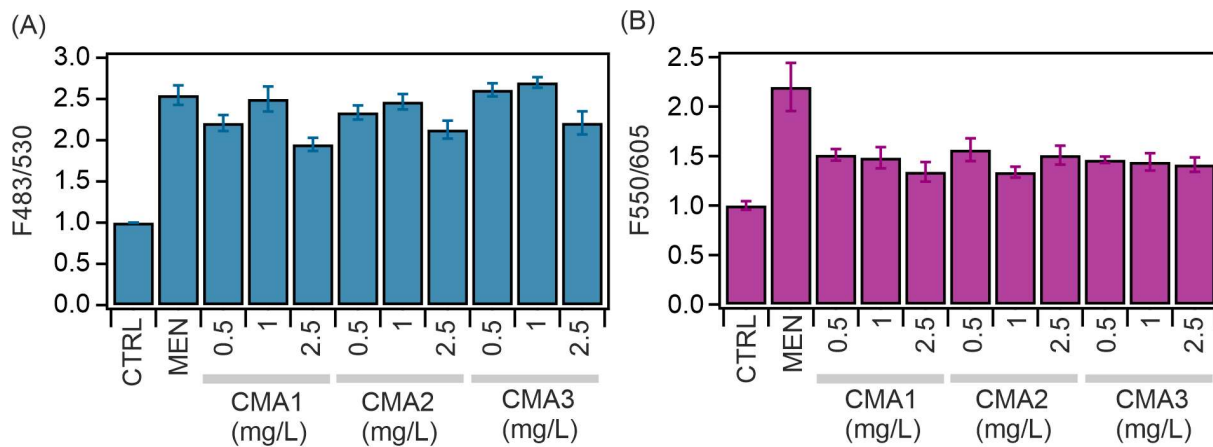


Fig. S5 Intracellular ROS scavenging activity of CMA1-3 samples in 0.5 – 2.5 mg/L concentration range (A). Intracellular superoxide radical ion dismutation activity for CMA1-3 samples in the 0.5 – 2.5 mg/L concentration range (B).

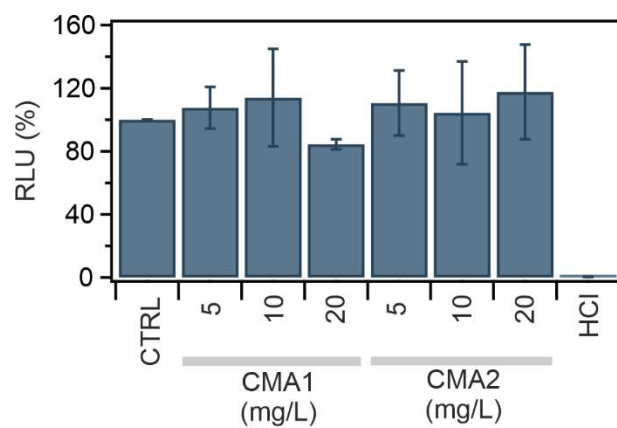


Fig. S6 Relative luminescence intensity measured in CellTiter Glo assay for CMA1 and CMA2 in 5 – 20 mg/L concentration range. CTRL means the negative, while HCl the positive control.

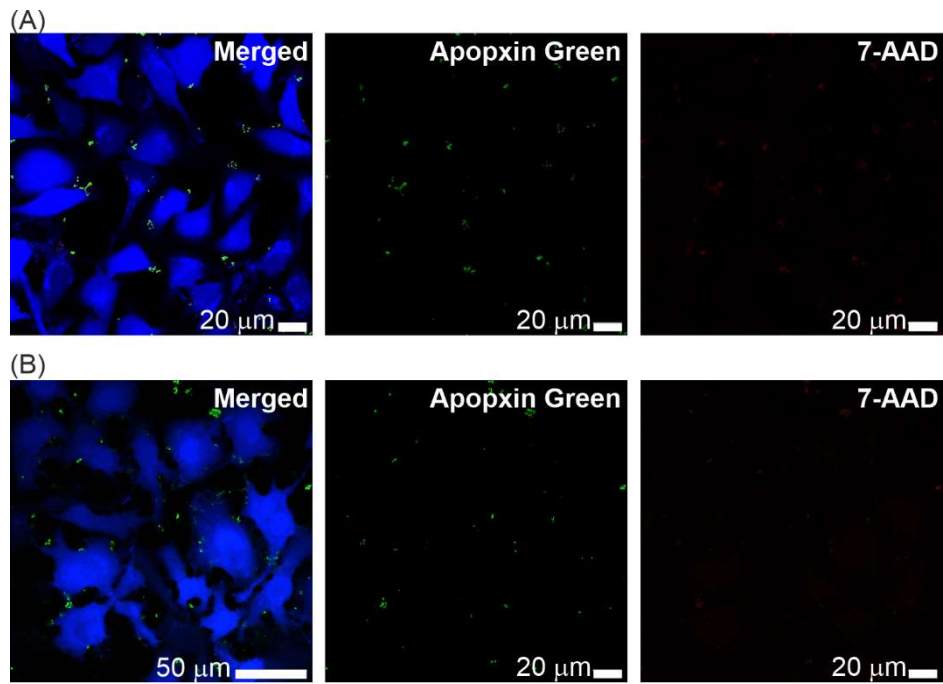


Fig. S7 Apoptosis/necrosis detection assay for un-treated (A) and 5mg/L CMA3-treated cells (B). Apopxin Green and 7-AAD fluorescent dyes labelled the live, apoptotic and necrotic cells. “Merged” labels denote their collective representation.

References

1. Z. P. Xu, G. Stevenson, C. Q. Lu and G. Q. Lu, *J. Phys. Chem. B*, 2006, **110**, 16923-16929.
2. W. H. Bragg and W. L. Bragg, *Proc. R. soc. Lond. Ser. A-Contain. Pap. Math. Phys. Character*, 1913, **88**, 428-438.
3. P. A. Hassan, S. Rana and G. Verma, *Langmuir*, 2015, **31**, 3-12.
4. N. Fairley, V. Fernandez, M. Richard-Plouet, C. Guillot-Deudon, J. Walton, E. Smith, D. Flahaut, M. Greiner, M. Biesinger, S. Tougaard, D. Morgan and J. Baltrusaitis, *Appl. Surf. Sci. Adv.*, 2021, **5**, 100112.
5. M. H. Hadwan and H. N. Abed, *Data Brief*, 2016, **6**, 194-199.
6. C. Beaucham and I. Fridovich, *Anal. Biochem.*, 1971, **44**, 276-287.
7. A. Szerlauth, Á. Varga, T. Madácsy, D. Sebők, S. Bashiri, M. Skwarczynski, I. Toth, J. Maléth and I. Szilagy, *ACS Mater. Lett.*, 2023, **5**, 565-573.
8. M. C. Biesinger, *Surf. Interface Anal.*, 2017, **49**, 1325-1334.
9. B. Li, J. Tang, W. Y. Chen, G. Y. Hao, N. Kurniawan, Z. Gu and Z. P. Xu, *Biomaterials*, 2018, **177**, 40-51.
10. G. Zhang, L. Wu, A. T. Tang, B. Weng, A. Atrens, S. D. Ma, L. Liu and F. S. Pan, *RSC Adv.*, 2018, **8**, 2248-2259.
11. J. Y. Zeng, C. P. Ding, L. Chen, B. Yang, M. Li, X. Y. Wang, F. M. Su, C. T. Liu and Y. J. Huang, *ACS Appl. Mater. Interfaces*, 2023, **15**, 378-390.
12. Y. Zhang, L. X. Chen, R. M. Sun, R. J. Lv, T. Du, Y. H. Li, X. M. Zhang, R. T. Sheng and Y. F. Qi, *ACS Biomater. Sci. Eng.*, 2022, **8**, 638-648.
13. X. Y. Liu, D. X. Li, Y. Liang, Y. Lin, Z. X. Liu, H. T. Niu and Y. H. Xu, *J. Colloid Interface Sci.*, 2021, **601**, 167-176.
14. Z. Liu, L. N. Xie, K. Q. Qiu, X. X. Liao, T. W. Rees, Z. Z. Zhao, L. N. Ji and H. Chao, *ACS Appl. Mater. Interfaces*, 2020, **12**, 31205-31216.
15. Y. Y. Huang, Z. Liu, C. Q. Liu, E. G. Ju, Y. Zhang, J. S. Ren and X. G. Qu, *Angew. Chem.-Int. Edit.*, 2016, **55**, 6646-6650.
16. S. Zhang, J. Chen, W. S. Yang and X. Chen, *Nano Res.*, 2022, **15**, 7940-7950.
17. B. Q. Wang, Y. Y. Fang, X. Han, R. T. Jiang, L. Zhao, X. Yang, J. Jin, A. J. Han and J. F. Liu, *Angew. Chem.-Int. Edit.*, 2023, e202307133.